

# PHYSICAL REVIEW B

## CONDENSED MATTER

THIRD SERIES, VOLUME 28, NUMBER 2

15 JULY 1983

### Interaction of hydrogen with a Pd(111) surface

W. Eberhardt,\* Steven G. Louie,<sup>†</sup> and E. W. Plummer

Department of Physics, University of Pennsylvania, Philadelphia, Pennsylvania 19104-3859  
and Laboratory for Research on the Structure of Matter, University of Pennsylvania,  
Philadelphia, Pennsylvania 19104-3859

(Received 26 January 1983)

The electronic properties of H chemisorbed on the Pd(111) surface are studied with the use of angle-resolved photoelectron spectroscopy and a self-consistent pseudopotential mixed-basis theoretical calculation. Adsorption of H onto a substrate cooled below  $\sim 250$  K results in an ordered  $(1 \times 1)\text{H}$  overlayer, deduced from the symmetry of the dispersion of the H-Pd bonding band, which is split off from the Pd bulk bands. A comparison between theory and experiment gives very good agreement when the H atoms occupy threefold surface sites with a H-Pd bond length of  $1.69 \text{ \AA}$ . The bonding is predominantly H  $1s$ -Pd  $4d$  as can be seen in the charge-density plots and the angular-momentum-decomposed local densities of states. Room-temperature adsorption of hydrogen or adsorption at low temperatures followed by a brief warming to  $\geq 270$  K produces a form of chemisorbed H which is nearly invisible in the photoelectron spectra. The possible bonding configurations of this invisible state are discussed.

#### I. INTRODUCTION

The interaction of H with the bulk of Pd has been investigated thoroughly due to the high solubility of H in Pd.<sup>1</sup> The nature of the adsorbed H and the relationship between adsorbed and dissolved H is not as well understood. For example, only a few years ago it was believed that the strongly chemisorbed H state could not be in equilibrium with the bulk,<sup>2</sup> instead a weakly bound adsorption state was postulated.<sup>3</sup> However, recent  $\text{H}_2$  molecular-beam experiments have shown that equilibrium between chemisorbed H and dissolved H below the surface (macroscopic dimensions) is reached rapidly at temperatures above  $300 \text{ K}$ .<sup>5</sup> There is some evidence from the low-energy electron diffraction (LEED) measurements of Christmann *et al.*<sup>6</sup> that the concentration in the first few layers may be larger than deep in the bulk.

Figure 1 shows a simple schematic potential-energy diagram for H and  $\text{H}_2$  interacting with a Pd surface. The potential-energy curve for the  $\text{H}_2$  molecule has a weak minimum near the surface, while the atomic H potential-energy curve has a deep minimum closer to the surface. The molecular and atomic curves cross leading to dissociation of the incoming  $\text{H}_2$  molecule. Engel and Kuipers showed that the curve crossing is below the zero of energy for gas phase  $\text{H}_2$ , so that dissociation is not activated on

Pd(111).<sup>5</sup> The atomic adsorption energy ( $E_{\text{ads}}$ ) for H on Pd(111) has been measured by Conrad *et al.*<sup>7</sup> to be  $0.46 \text{ eV}$  at low coverages, while the heat of solution in the bulk ( $\Delta\bar{H}$ ) is  $0.20 \text{ eV}$ .<sup>1</sup> The chemisorbed H is bound much more tightly than the dissolved H, but the depth of this surface well will depend upon the H concentration on the surface. Engel and Kuipers showed that one analysis of their molecular-beam data predicted a variation in the adsorption energy of a H atom as a function of H concentration on the surface, dropping from  $0.46 \text{ eV}$  at low cover-

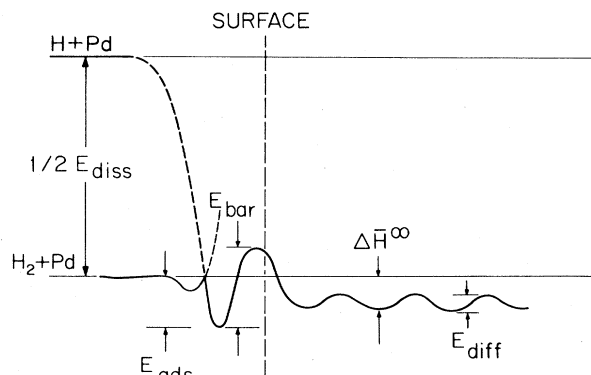


FIG. 1. Schematic potential-energy diagram as a function of distance from the surface.  $E_{\text{diss}}$  is the gas phase  $\text{H}_2$  dissociation energy.

age to 0.4 eV near saturation.<sup>5</sup> According to their work, the low-coverage H was disordered while the high-coverage layer was ordered. Behm *et al.*<sup>8</sup> reported that for H adsorbed on Pd(100) at 170 K, the adsorption energy was constant up to about 0.9 of a monolayer, then fell by 30% when the coverage was increased to 1.3 of a monolayer, due presumably to repulsive H-H interactions.

The actual potential-energy diagram for the interaction of H with Pd could be considerably more complicated than indicated by Fig. 1. For chemisorbed atoms such as H on Pd or O on Ni, where it is known that they dissolve into the bulk, there may be a deep potential well slightly underneath the surface. This has been postulated by Andersson<sup>9</sup> to explain the vibrational spectra of  $p(2 \times 2)O$  and  $c(2 \times 2)O$  on Ni(100) and by Eberhardt *et al.*<sup>10</sup> to explain H adsorption on Ni, Pd, and Pt. If the analysis of Engel and Kuipers<sup>5</sup> of the LEED data of Christmann *et al.*<sup>6</sup> is correct, then there is an abnormally high concentration of H in the surface region for room-temperature adsorption. This indicates that the potential well at the second or third layer of Pd must be different than the equivalent potential well deep inside of the bulk.

Conrad *et al.*<sup>7</sup> have shown that the adsorbed H can be identified from the kinetics of desorption and the work-function change. The adsorption of H onto a Pd (111) crystal at room temperature resulted in a thermal-desorption spectrum with a single-surface desorption peak at  $\sim 380$  K and a broad higher-temperature desorption peak from the dissolved H. Saturated H caused a 0.18-eV work-function increase while dissolved H gave no work-function change.<sup>7</sup> If the substrate temperature is decreased below room temperature, more H is adsorbed. The beam work of Engel and Kuipers indicate that the surface coverage increased as the substrate was cooled.<sup>5</sup> The concentration saturated at 250 K.<sup>5</sup> No thermal-desorption spectra have been reported for substrate temperatures below room temperature, but presumably the thermal-desorption spectra will look like other single crystal faces of Ni and Pd, with two desorption peaks.<sup>11</sup> The high-temperature peak will be present for low coverages while the low-temperature peak (below room temperature) will appear in the thermal-desorption spectra for higher coverages.

At the present time there is very little information available concerning the degree of order of H adsorbed onto Pd surfaces. Christmann *et al.*<sup>6</sup> observed no new diffraction spots in their LEED experiment for H adsorbed on Pd(111) at room temperature. The background intensity decreased upon adsorption of H indicating an ordered overlayer, presumably a  $(1 \times 1)$  structure.<sup>6</sup> In contrast to the LEED study, molecular-beam experiments<sup>5</sup> showed that H adsorbed at room temperature was disordered while adsorption at  $T < 250$  K lead to an ordered overlayer. The easiest interpretation of the molecular-beam experiment is that low-coverage H is disordered while a high-coverage layer is ordered.<sup>5</sup> Christmann *et al.*<sup>6</sup> have observed that high exposures of H ( $10^{-5}$  Torr) at room temperature produces a measurable shift in the voltage maximum in the substrate LEED beams, consistent with a 2% expansion of the Pd-Pd interplanar distance.

The objectives of this study are threefold.

(1) To identify the surface states or resonances on clean Pd(111) and to measure their dispersion in the two-

dimensional surface Brillouin zone (SBZ). This data can be compared to existing theoretical calculations.<sup>13-15</sup> Several experimental papers have shown dramatic changes in the  $d$ -band region of the photoemission spectra from Pd(111) upon adsorption of a foreign atom or molecule.<sup>10,16-19</sup> The latter observation is a clear sign of surface states or resonances.

(2) To measure the position in energy and dispersion of the H-induced energy levels when H is adsorbed in an ordered array into a cooled Pd substrate.<sup>5</sup> These measurements can be compared to theoretical calculations to determine the bonding site and the nature of the chemisorbed state.<sup>13,20</sup>

(3) To investigate the nature of the H-Pd bond at higher substrate temperatures of lower coverages where molecular-beam data indicate that the H layer is disordered.<sup>5</sup>

There have been three previous photoemission studies of H adsorbed on Pd(111). Demuth<sup>16</sup> exposed a Pd(111) crystal at 80 K to 2 L of  $H_2$ , resulting in a work-function change of 0.18 eV [1 langmuir =  $1 \text{ L} \equiv 10^{-6}$  Torr sec]. The resulting changes in the angle-integrated photoemission spectrum were a new H  $1s$ -Pd bonding level 6.4 eV below the Fermi energy and a quite dramatic loss of intensity in the  $d$ -band region within 3 eV of the Fermi energy. Conrad *et al.*<sup>17</sup> measured the changes in the angle-integrated photoemission spectra when  $10^{-6}$  Torr pressure of  $H_2$  was introduced into the chamber, with the crystal at 200 K. They observed a H  $1s$ -Pd bonding orbital at 6.5 eV below  $E_F$  and larger changes in the  $d$ -band emission near the Fermi energy. The decrease in  $d$ -band emission near the Fermi energy in both studies indicates that surface states or resonances are being quenched by H adsorption.<sup>15</sup> Weng and El-Batanouny studied H adsorption onto Pd layers grown on a Nb crystal at room temperature.<sup>19</sup> Their angle-integrated photoemission results indicate that an intrinsic surface state near the Fermi energy is destroyed by H adsorption.

In an earlier paper Louie compared the calculated changes in the density of states induced by a  $H(1 \times 1)$  layer on Pd(111) to the measured angle-integrated photoemission difference curves.<sup>13</sup> The conclusion was that H was bound in a threefold site on the surface, for the specific conditions of Demuth's experiment: 2-L exposure at 80 K.<sup>16</sup> This comparison undoubtedly ruled out a terminally bonded configuration for the H atoms, but it was impossible to distinguish between the two different threefold sites or to accurately determine the Pd-H bond length. The work of Feibelman, Hamann, and Himpfel,<sup>21</sup> who determined the bonding site of H on Ti(0001), clearly illustrates the pitfalls of using angle-integrated photoemission data. Their first paper compared theoretical calculations for different geometries with the angle-integrated data of Eastman.<sup>22</sup> They concluded that the H was bound in a threefold site which was the natural extension of the hcp lattice with a Ti-H bond length of 1.78 Å.<sup>23</sup> Subsequent to the publication of this paper, Himpfel measured angle-resolved photoemission spectra from H on Ti(0001).<sup>21</sup> The best theoretical fit to this data was for a threefold site in the fcc continuation of the lattice with a Ti-H bond length of 1.90 Å.<sup>21</sup> The bond length and site changed using angle-resolved data compared to angle-integrated data.

## II. EXPERIMENTAL AND THEORETICAL PROCEDURES

### A. Experiment

The experiments were performed at the Synchrotron Radiation Center of the University of Wisconsin. The synchrotron light was dispersed by a dual toroidal grating monochromator which operated in the  $10^{-11}$  Torr vacuum range. The angle-resolving detector is a 2.5-cm mean radius hemispherical analyzer with an angular resolution of  $\pm 2.5^\circ$ . The combined resolution of the monochromator and analyzer was usually set at a few tenths of an eV. The main vacuum chamber operated in the low  $10^{-10}$  Torr range. The sample was mounted onto a Dewar with two-axis rotation and  $x, y, z$  translation. With liquid- $N_2$  cooling, the crystal could be cooled to  $\sim 100$  K or heated resistively to 1000 K. The temperature was measured by a thermocouple spot welded directly to the Pd crystal.

The Pd(111) crystal was loaned to us by Nilsson. The crystal, which had previously been extensively cleaned, was cleaned in our chamber by repeated sputter-annealing cycles. The orientation of the SBZ mirror planes with respect to the direction of the light polarization was determined by symmetry-related angle-resolved photoemission measurements. Work-function changes were measured by recording the shift in the cutoff of the secondary electrons in the photoemission-energy distribution. The sample was usually biased by several volts negative to avoid any problems with differences in work function between the crystal and analyzer. Crude thermal-desorption spectra were recorded by instantaneously flipping on the Variac used to heat the crystal. The pressure change was measured by the ion gauge or a mass spectrometer. The temperature versus time was nearly linear.

### B. Theory

The calculation procedure employed here has been described elsewhere.<sup>13,15,24</sup> It is a self-consistent pseudopotential scheme utilizing a local-density description of the exchange and correlation potential energy. The  $d$  and  $s$  bands are treated in a mixed-basis technique using plane waves plus  $d$ -like Gaussians.<sup>24</sup> The calculation is done for a seven-layer slab of Pd with a  $(1 \times 1)$ H layer bound to each side. A vacuum region equivalent to four atomic layers of Pd separates each slab, where the whole calculation is done in a supercell description.<sup>13,25</sup> The only inputs to the calculation are the atomic positions of the H and Pd and the bare ionic pseudopotentials for the  $Pd^{10+}$  and  $H^{1+}$  ion cores. Convergence was achieved with  $\sim 300$  plane waves and 35 local orbitals (five for each Pd atom). Calculations of the critical points in the bulk band structure of Pd using this technique agree quite well with measured values.<sup>24</sup>

The Pd-Pd interplanar spacing at the surface was assumed to be the same as the bulk spacing. Ion scattering experiments on Ni(111) (Refs. 26 and 27) and Pt(111) (Ref. 28) indicate little or no change in the surface-lattice spacing before or after H adsorption at low temperature. The H was assumed to be in a  $(1 \times 1)$  ordered configuration and only the site and bond length were varied. Compar-

ison to angle-integrated photoemission results ruled out the terminal site.<sup>13,16</sup>

The electronic states for clean Pd(111) (Ref. 15) and H adsorbed in a  $(1 \times 1)$  configuration into the two different trigonal sites were calculated. The two sites differ in the stacking sequence, for the fcc structure there is an  $abcabc$  sequence while a hcp structure has an  $abab$  sequence. Several different Pd-H spacing centered about 1.69 Å (which is the sum of the metallic radius and H covalent radius) were used. Normal-mode analysis of the vibrational modes of H adsorbed on Ni(111) and Pt(111) indicates that the metal-H spacing is given by the covalent metallic radius.<sup>29</sup> A LEED analysis for a  $p(2 \times 2)$ H on Ni(111) structure yielded a much longer H-Ni bond distance (1.84 Å) than deduced from the vibrational spectra.<sup>30</sup> The analysis of the H on Ti(0001) angle-resolved data also deduced a long Ti-H bond length.<sup>21</sup>

In comparing the angle-resolved difference curves and the calculated  $k$ -resolved change in the density of states, the theoretical difference curve was defined as

$$\Delta N(\vec{k}, E) = \sum_i \int_{-\infty}^{E_F} \Delta n_i(\vec{k}, E') f(E - E', \gamma(E)) dE', \quad (1)$$

where  $\Delta n_i(\vec{k}, E)$  is the difference between the local density of states at  $\vec{k}$  for the chemisorbed surface and the clean surface at the  $i$ th layer. The total change in the density of states as defined in Ref. 13 is the integral of  $\Delta N(\vec{k}, E)$  over the SBZ. The function  $f(E - E', \gamma(E))$  accounts for the lifetime broadening and instrument resolution.  $f$  is a Gaussian function with an energy-dependent width adjusted empirically,

$$\gamma(E) = 0.15 |E - E_F| + 0.2, \quad (2)$$

measured in eV. Equation (1) approximates the actual angle-resolved photoemission difference curves. It ignores final-state and matrix-element effects so that the intensities should not be expected to correspond to experimental data.

## III. RESULTS

### A. Clean Pd and H(1 × 1)-Pd

The identification of a surface state on Pd is complicated by the complexity of structure seen in the photoemission spectra due to direct bulk transitions. These direct transitions from the occupied  $d$  bands produce multiple peaks in a spectrum over an energy range of 3 or 4 eV below the Fermi surface.<sup>13,24</sup> This bulk structure moves in energy with changing photon energy or collection angle making an unambiguous identification of a surface state or resonance difficult. A surface state or resonance is a two-dimensional state, so that its energy in a spectrum should be independent of  $k_{\parallel}$  if  $k_{\perp}$  is held fixed. It should also be sensitive to the adsorption of a foreign atom or molecule.

Figures 2(a), 3(a), and 4(a) each show three sets of angle-resolved energy distributions for clean Pd(111) and saturated H adsorption at  $\sim 100$  K. Spectra for three photon energies (30, 40, and 50 eV) are shown on each figure for the three high-symmetry points of the SBZ (see top

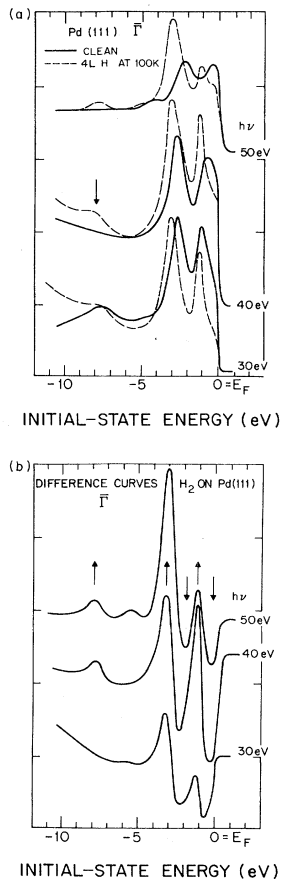


FIG. 2. (a) Normal-emission spectra from Pd(111) and  $4 \times 10^{-6}$  Torr sec exposure of  $H_2$  at 100 K. (b) Difference curves for the three sets of spectra shown in (a). Arrows pointing up are H-induced states, arrows pointing down are intrinsic surface states or resonances.

of Fig. 5). Three observations are obvious: (1) there is a lot of structure in the clean spectra in the first 4 eV below the Fermi energy; (2) this structure changes quite dramatically with H adsorption; (3) a new H-induced level appears below the  $d$  band of Pd. This peak, which is 7.9 eV below  $E_F$  at the SBZ center ( $\bar{\Gamma}$ ), 6.4 eV below  $E_F$  at  $\bar{M}$ , and 5.9 eV below  $E_F$  at  $\bar{K}$ , is marked by the arrows in Figs. 2(a), 3(a), and 4(a).

The dispersion of this H-Pd split-off band can be used to determine the symmetry of the H overlay unit cell. Figure 5(b) shows the measured dispersion of the split-off state as a function of  $k_{\parallel}$  in the two high-symmetry directions of the clean SBZ. The direction from  $\bar{\Gamma}$  to  $\bar{M}$  returns to  $\bar{\Gamma}$  in the second zone, so the dispersion should repeat around  $\bar{M}$  if the H structure is  $(1 \times 1)$ . The figure shows that in this direction the dispersion is symmetric about  $\bar{M}$ . Going in the  $\bar{\Gamma}$  to  $\bar{K}$  direction of the SBZ, the dispersion should not be symmetric about the zone corner  $\bar{K}$ . Along this direction in the SBZ the path goes  $\bar{\Gamma}$  to  $\bar{K}$  to  $\bar{M}$  then back to  $\bar{K}$  (see top of Fig. 5). The measured dispersion in this direction is plotted in Fig. 5(b) and exhibits the correct dispersion. Exposures of 2 L or more at

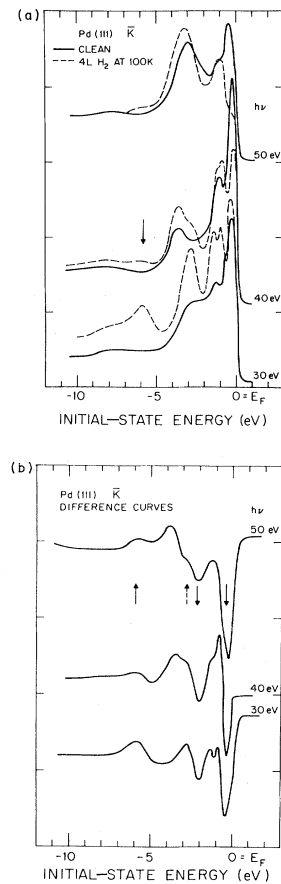


FIG. 3. (a) Photoemission spectra at  $\bar{K}$  in SBZ for clean and H adsorption at 100 K. The collection angle was adjusted at each photon energy to keep  $k_{\parallel}$  fixed for an initial energy of  $-3$  eV. (b) Difference curves corresponding to the curves in (a).

$\sim 100$  K gave this  $H(1 \times 1)$  dispersion.

The fact that H forms an ordered  $(1 \times 1)$  structure makes the analysis of the photoemission curves in Figs. 2(a), 3(a), and 4(a) easier. A  $(1 \times 1)$  layer cannot fold the structure back with a smaller surface reciprocal-lattice vector than the clean surface, or scatter strongly emitting angular regions into the detection direction. This means that it is possible to interpret angle-resolved difference curves. These difference curves are shown in Figs. 2(b), 3(b), and 4(b). Armed with the difference curves, our criteria for identifying a surface state or resonance are as follows: (1) the structure is sensitive to H adsorption; (2) the energy of the structure is independent of photon energy; (3) the structure can be identified in the actual energy distributions as well as in the difference curves. This assures that the difference curves do not produce peaks due to inelastic scattering from the adsorbate, filling in minimum in the clean spectra.

A negative peak in the difference curves indicates an intrinsic surface state while a positive peak marks an extrinsic H-induced state. Our first analysis of Figs. 2–4 will be strictly experimental. We will then compare the differ-

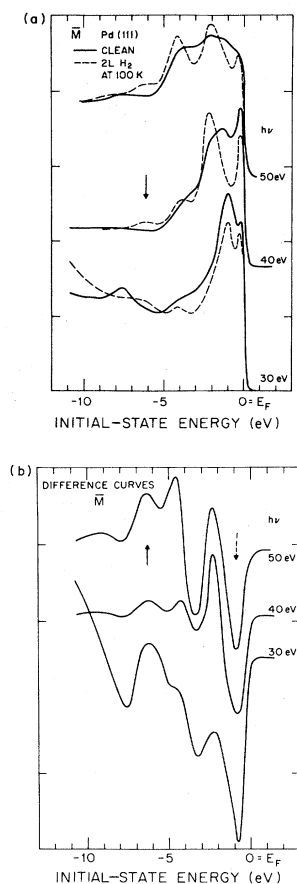


FIG. 4. (a) Photoemission spectra at  $\bar{M}$  in the SBZ for clean and H adsorption at 100 K. The collection angle was adjusted at each photon energy to keep  $k_{\parallel}$  fixed for an initial energy of  $-3$  eV. (b) Difference curves corresponding to the curves in (a).

ence curves to calculated changes in the  $k$ -resolved density of states.

The normal-emission spectra and difference curves shown in Fig. 2 are the easiest to analyze. All three difference curves show basically the same structure except for

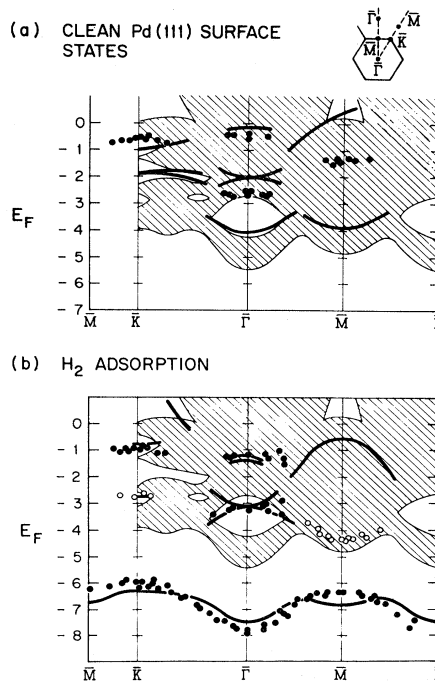


FIG. 5. Calculated and measured surface states for (a) Pd(111) and (b) H(1 $\times$ 1) Pd(111) (Ref. 13). The shaded regions are the calculated projection of the bulk bands onto the (111) surface. The solid lines are calculated surface states or resonances, the solid circles are data. The open circles indicate peaks with some uncertainty.

the intensity of the H 1s split-off state, which is very weak at  $\hbar\omega = 30$  eV. The peak in the clean  $\hbar\omega = 30$  eV spectrum at approximately  $-8$  eV is caused by a high density of states in the final states of Pd, in agreement with optical-absorption data.<sup>31</sup> This structure remains at a constant kinetic energy as the photon energy is changed. There are two clear intrinsic surface states [negative peaks in Fig. 2(b)] at energies  $-0.3$  and  $-2.2$  eV, and three visible extrinsic H-induced states at  $-1.2$ ,  $-3.1$ , and  $-7.9$  eV. In all these cases one can easily see the appropriate structure in the energy distributions of Fig. 2(a). The  $-0.3$ -eV in-

TABLE I. Intrinsic surface states or resonances on Pd(111). LCAO is the linear combination of atomic orbitals. (An asterisk denotes tentative values.)

Symmetry point	Experimental energy eV	Theoretical energy		Type of state
		Pseudopotential <sup>a</sup> eV	LCAO <sup>b</sup>	
$\Gamma$	$> -0.3$	$-0.2$	$-0.07$	$d_{xy}, d_{zx}$
	$-2.2$	$-2.0$	$-2.28$	$d_{x^2-y^2}, d_{xy}$
		$-4.1$	$-4.06$	$d_{3z^2-r^2}, s$
$\bar{K}$	$> -0.3$	$-1.0$	$-0.49$	$d_{zx}, d_{zy}$
	$-2.1^*$	$-1.9$	$-1.44$	$d_{x^2-y^2}, d_{xz}$
		$-3.0$	$-3.8$	backbone
$\bar{M}$			$-0.18$	$d_{xy}, d_{x^2-y^2}$
	$\sim 1$	$-3.8$	$-4.16$	$s, d_{x^2-y^2}, d_{xy}$

<sup>a</sup>Reference 13.

<sup>b</sup>Reference 14.

TABLE II. Extrinsic  $H(1 \times 1)$ -induced surface states or resonances on Pd(111). (An asterisk denotes tentative experimental identification or identification via comparison with theory.)

Symmetry points	Experimental energy	Theory pseudopotential <sup>a</sup>
$\bar{\Gamma}$	-1.2 eV	-1.3 eV
	-3.1 eV	-1.4 eV
	-7.9 eV	-3.2 eV
$\bar{K}$	-1.0 eV	-7.5 eV
	-2.8 eV*	-0.8 eV
	-5.9 eV	-2.8 eV
$\bar{M}$	-4.1 eV*	-6.3 eV
	-6.4 eV	-0.6 eV
		-6.8 eV

<sup>a</sup>This theoretical calculation is for a  $H(1 \times 1)$  layer in an hcp structure with the Pd-H bond length at 1.69 Å (Ref. 13).

trinsic surface state or resonance may be closer than 0.3 eV to the Fermi energy since our resolution in these experiments was  $\sim 0.2$  eV. There is a weak structure visible at  $\sim 5.5$  eV in the  $\hbar\omega = 30$  and 50 eV difference curves. This structure is not visible in the actual energy distributions, so we disregard it. Tables I and II list the intrinsic and extrinsic surface states or resonances observed in these experiments. The values listed with an asterisk are tentative or only identified via comparison to theoretical calculations.

Lloyd *et al.*<sup>18</sup> have published a normal-emission difference curve for CO adsorption on Pd(111). Their curve shows two negative peaks at -0.8 and -2.1 eV. The -2.1-eV peak agrees quite well with our results, but -0.8 eV is a little farther from the Fermi energy than we observe. The CO-induced features in the normal-emission difference curve are quite different from those shown in Fig. 2(b), as would be expected.<sup>18</sup>

Figures 3(a) and 3(b) show the energy distributions and difference curves taken at the  $\bar{K}$  point of the SBZ. The H 1s-Pd split-off state is most visible at  $\hbar\omega = 30$  eV with an energy of -5.9 eV. Again there is a marked attenuation of the intensity at the Fermi energy upon H adsorption. Comparison of Figs. 3(a) and 3(b) shows that there is an intrinsic surface state or resonance at -0.3 eV, but the dip at -2.0 eV in Fig. 3(b) does not correspond to a peak in the clean spectra. There are clear extrinsic states at  $\sim -1.0$  and -5.9 eV. The structure at -2.8 eV we consider as tentative.

The data at  $\bar{M}$  shown in Figs. 4(a) and 4(b) are by far the most confusing. There are dramatic changes in the energy distributions, but the changes are not the same for the different photon energies. The only clear feature is the weak split-off state at -6.4 eV. There is a simple explanation for this behavior. There are two different  $\bar{M}$  points ( $\bar{M}$  and  $\bar{M}'$ ) when the three-dimensional bulk structure is superimposed on the two-dimensional SBZ, because the solid only has trigonal symmetry. At a given photon energy, the peaks in photoemission spectra at  $\bar{M}$  and  $\bar{M}'$ , due to bulk transitions, will come from different parts of

the band structure and consequently will appear at different initial-state energies. But  $\bar{M}$  and  $\bar{M}'$  are connected by a surface reciprocal-lattice vector, so the bulk transitions seen at  $\bar{M}'$  can be "umklapped" from  $\bar{M}$ . The adsorption of H must increase or decrease the amount of umklapp. Judging from the better definition of peaks in the  $H(1 \times 1)$  spectra of Fig. 4(b), H seems to decrease the surface umklapp process. The surface must be electronically smoother with the H adsorbed than it is clean. This umklapp process makes the difference curves at  $\bar{M}$  useless. The only reasonable approach is to look for peaks in the energy distributions which are independent of photon energy. The -4.1-eV peak in the H adsorption spectra appears in all of the curves, but it also seems to be present in the clean spectra. There is a sharp peak near the Fermi energy, but it also appears in both the clean and adsorption spectra.

Figure 5 shows the comparison of the clean and H-induced features in the experimental data with the theoretical calculations. The extrinsic H-induced features in Fig. 5(b) show remarkable agreement between theory and experiment except near  $\bar{M}$  where we have experimental difficulty identifying H-induced features. The symmetry of the H split-off state proves that we are looking at a  $(1 \times 1)$ -ordered H overlayer. The agreement between theory and experiment for the intrinsic surface states [Fig. 5(a)] is not quite as good as it is for the H-induced features.

With the angle-resolved difference curves shown in Figs. 2(b) and 3(b), the previously reported angle-integrated difference curves<sup>16,17</sup> can be interpreted.<sup>13</sup> These angle-integrated curves show five features: positive peaks at -6.4, -3.2, and -1.6 eV, and negative peaks at -0.4 and -2.2 eV. The -6.4-eV peak is the  $k$  average over the split-off H state which disperses from -7.9 eV at  $\bar{\Gamma}$  to -5.9 eV at  $\bar{K}$ . The -3.2-eV peak is the strong H-induced level seen in normal emission at -3.1 eV and at -2.8 eV at  $\bar{K}$ . The -1.6-eV H-induced level is seen at -1.2 at  $\bar{\Gamma}$  and -1.0 eV at  $\bar{K}$ . The two negative peaks in the angle-integrated spectra can be seen in the difference curves at  $\bar{\Gamma}$  and  $\bar{K}$ .

The calculated results for H adsorbed at three different geometries are presented in Figs. 6-9. These results were obtained with the H-Pd bond length set at 1.69 Å which is the sum of the Pd metallic radius and the H covalent radius. In addition to the top site, the two threefold sites corresponding to a fcc stacking position (the  $B$  site) and a hcp stacking position (the  $C$  site) were considered. We find that the theoretical spectra for the two threefold sites are both in excellent agreement with angle-integrated and angle-resolved photoemission data. The sensitivity of the calculation was tested by varying the H-Pd interplanar distance about the 1.69-Å value. The energy positions of the H-induced features were found to be rather insensitive to small variations in this parameter.<sup>32</sup> It should be stressed again that the calculated curves in Figs. 6-9 do not include any photoemission matrix-element effects.

Figures 6 and 7 depict the calculated  $\vec{k}$ -resolved difference curves  $\Delta N(\vec{k}, E)$  at  $\bar{\Gamma}$  and  $\bar{K}$ , respectively, for the three chemisorption sites. The theoretical results clearly rule out the top site as the chemisorption position for the low-temperature phase. The dashed curve in Fig. 6 (Fig. 7) is the sum of the three difference curves in Fig. 2(b)

[Fig. 3(b)]. Comparison of the theoretical and experimental results for  $\vec{k}=\bar{\Gamma}$  (Fig. 6) and  $\vec{k}=\bar{K}$  (Fig. 7) shows a truly remarkable agreement for the two threefold sites. In fact, the few disagreements between theory and experiment depicted in Fig. 5 are not obvious discrepancies in Figs. 6 and 7. For example, the theoretical clean-surface state at  $-4$  eV at  $\bar{\Gamma}$  is only a small dip in the theoretical difference curves which would be hard to see experimentally. Both threefold geometries yield virtually identical surface spectra because the predominate changes in electronic structure upon chemisorption are a result of the interaction of the H  $1s$  orbital with the Pd  $d$  orbitals. These interactions give rise to modifications and creations of surface states which are almost completely localized on the H atoms and the surface Pd atoms. Thus the arrangement of the subsurface layer atoms which distinguishes the two threefold sites does not play a role in determining the  $\Delta N$ 's.

From the theoretical results we can now explain the physical origins of all the structures in the measured spectra [Figs. 2(b) and 3(b)]. For example, for the C-site geometry, the three negative valleys in the  $\vec{k}=\bar{\Gamma}$  difference curve correspond to the removal (bonding away or shifting to lower-energy positions) of the intrinsic surface states at energies  $-0.2$ ,  $-2.0$ , and  $-4.1$  eV, and the positive peaks correspond to the appearance of the extrinsic H-induced states at  $-1.3$ ,  $-1.4$ ,  $-3.2$ , and  $-7.5$  eV. An analysis of the wave functions of the electrons shows that the extrinsic states at  $-1.3$ ,  $-1.4$ , and at  $-3.2$  eV are merely the same states (in character) as the intrinsic states at  $-0.2$  and  $-2.0$  eV, respectively, but they have been shifted to higher binding energies as a consequence of changes in the surface potential due to the presence of the H atoms. The intrinsic surface state at  $-4.1$  eV for the clean surface, on the other hand, is combined with the

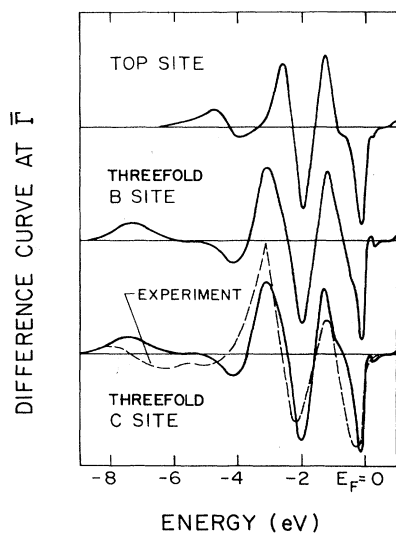


FIG. 6. Calculated angle-resolved difference curves for H adsorption with  $\vec{k}=\bar{\Gamma}=0$ . The three sites are on top and the two different three fold sites (*B* for fcc stacking and *C* for hcp stacking) follow. The H is ordered in a  $(1 \times 1)$  structure. The dashed curve is the sum of the three difference curves of Fig. 2(a).

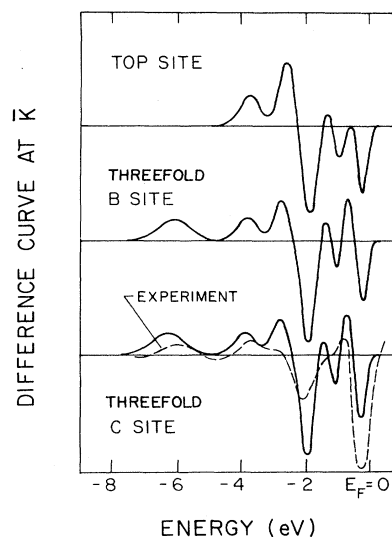


FIG. 7. Calculated angle-resolved difference curves for a  $H(1 \times 1)$  structure on Pd(111) with  $\vec{k}=\bar{K}$ . The dashed curve is the sum of the three difference curves of Fig. 3(a).

H  $1s$  orbital to form the H-Pd bonding adsorbate state at  $-7.5$  eV. Similar kinds of changes in the surface electronic structure occur at  $\bar{K}$ . Intrinsic surface states at  $-1.0$  and  $-1.9$  eV are removed forming the two valleys observed in the difference curves. Extrinsic surface states at  $-0.8$  and  $-2.8$  eV together with a H-Pd adsorbed bonding state at  $-6.3$  eV are created. The calculation further indicates that the large negative amplitude near  $E_F$  is due to modifications of weak surface resonances and bulk-state density near the  $d$ -band edge rather than removable bona fide intrinsic surface states.

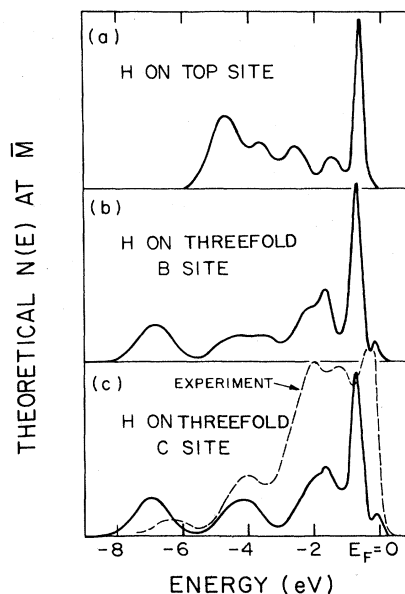


FIG. 8. Calculated angle-resolved density of states for  $H(1 \times 1)$  on Pd(111) with  $\vec{k}=\bar{M}$ . The dashed curve is the sum of the three H adsorption spectra in Fig. 4(a).

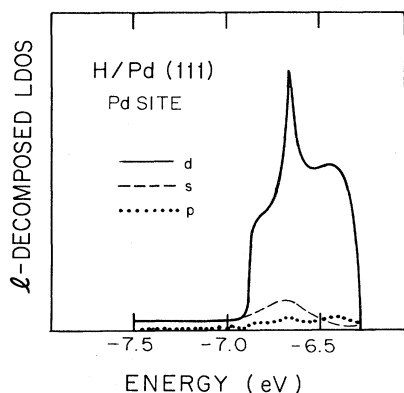


FIG. 9. Angular momentum decomposition of the local density of states on the surface Pd atom in the energy range of the split-off chemisorption band.

As discussed earlier, it is difficult to interpret difference curves for  $\vec{k}=\vec{M}$  because of surface umklapp processes. Thus we present in Fig. 8 the calculated  $N(E)$  at  $\vec{M}$  for comparison with experimental spectra shown in Fig. 4(a). The threefold site results produce most of the salient features observed in the experimental curves. In particular, there is one peak at  $-6.8$  eV corresponding to the H-Pd bonding state (experimental value is at  $-6.4$  eV) and three peaks located at  $-0.6$ ,  $-1.8$ , and  $-4.1$  eV in the theoretical curve. The two threefold sites produce the H-Pd bonding state split off from the Pd band at  $-6.8$  eV. The on-top site does not have a bonding state below the bottom of the Pd bands. The dashed curve at the bottom of Fig. 8 is the sum of the three energy distributions plotted in Fig. 4(a), with an appropriate inelastic background subtracted. Ignoring intensity variations, the experimental and theoretical curves qualitatively agree with the split-off state, the peak at  $\sim -4$  eV, and the broad band near  $-2$  eV. There is no sign in the experimental data of the sharp surface-state peak at  $-0.6$  eV predicted theoretically. This extrinsic surface state at  $\vec{M}$  is the only clear example where the theory and experiment disagree. The extrinsic surface band that we identified in Figs. 4 and 5 at  $\vec{M}$ , 4 eV below the Fermi energy, appeared to be in disagreement with the theoretical calculations, but Fig. 8 shows that this peak is in both the experimental data and the theoretical calculations. It is only a question of the theoretical definition of a surface state or resonance.

The theoretically predicted surface states for the clean surface and the H-adsorbed (in the three-fold  $C$  site) surface are summarized in Tables I and II together with the measured surface features. The excellent agreement between theory and experiment gives us much confidence in our theoretical methods and shows that the most likely geometry for the low-temperature phase is indeed with H on a threefold site at a H-Pd bond length of  $1.69$  Å. Our theoretical results further show that the surface electronic structure is practically the same for H on either the hcp or the fcc sites.

The nature of the chemisorption bond for this system may be studied in detail by examining the wave functions of the electrons in the H-Pd bonding band. In Fig. 9 we

present the  $l$ -decomposed local density of state  $D_l(E)$  for the Pd surface atom for this split-off chemisorption band.  $D_l(E)$  is defined by

$$D_l(E) = 2 \sum_k \int_{\Omega} \psi_k^*(r) P_l \psi_k(r) d^3r \delta(E - E_k), \quad (3)$$

where  $\Omega$  is a sphere with radius  $R = 1.0$  Å centered on a surface Pd atom. As seen from Fig. 9, the predominant harmonic components of this band at the Pd site is the  $d$  component. The choice of a particular radius  $R$  is somewhat arbitrary. However, a 25% change in  $R$  only results in a  $\sim 10\%$  change in the  $d$  component, favoring more  $d$  character at smaller  $R$ . Since the Pd-H distance is  $1.69$  Å, we feel that  $R = 1$  Å is a good physical choice. A similar calculation shows that the dominant component is the  $s$  wave at the H site. These results thus illustrate clearly and quantitatively our conclusion that the chemical bonding at this surface is mainly between the H  $1s$  orbital and the Pd  $4d$  orbitals.<sup>13,20</sup>

All of the previous experimental and theoretical discussions have concerned a saturated H exposure at a crystal temperature of  $\sim 100$  K. In Fig. 10 we show the evolution of the normal-emission spectra as a function of exposure or coverage. There are three important features illustrated by these spectra: (1) The surface state near the Fermi energy [see Fig. 5(a)] is extremely sensitive to adsorbed H.  $\frac{1}{4}$ -L exposure completely removes this state; (2) the H  $1s$ -Pd split-off state appears in the spectra at low exposures and grows in intensity as the exposure increases; (3) the energy of the split-off state shifts as the coverage changes. At  $\frac{1}{4}$ -L exposure the split-off state is  $\sim 7$  eV below the Fermi energy and it moves deeper as the cover-

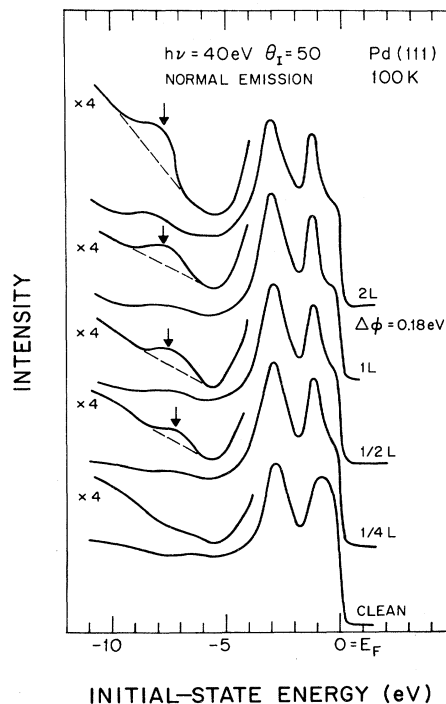


FIG. 10. Normal-emission photoemission spectra as a function of H exposure.

age increases. The split-off state reaches its maximum intensity and depth at  $\sim 2$ -L exposure. The shift in the binding energy of this peak in normal emission is undoubtedly a result of the loss of dispersion at low coverages. This could be a consequence of disorder at low coverage or because the island size is too small. The average energy of the two-dimensional band shown in Fig. 5(b) is  $-6.4$  eV. Therefore even at an exposure of  $\frac{1}{4}$  L there is still a small amount of dispersion, indicating that in the low-coverage regime the H is probably ordered in islands.

### B. Comparison with bulk Pd hydride

In this section we will compare our spectra and calculations for the surface of Pd with and without H present in the spectra, and calculations for bulk Pd and Pd hydride. There are numerous theoretical calculations of Pd hydride<sup>33</sup> which agree with each other in most qualitative features. On the other hand, the experimental situation was quite confusing<sup>34</sup> until the recent work of Schlapbach and Burger<sup>35</sup> and Bennett and Fuggle.<sup>36</sup> The x-ray photoelectron spectroscopy (XPS) data from these two groups for Pd and PdH<sub>x</sub> ( $0.6 \leq x \leq 0.8$ ) are in excellent agreement.

In Fig. 11 we have displayed the XPS data of Bennett and Fuggle<sup>36</sup> for Pd and PdH<sub>0.8</sub>. The Pd hydride was prepared by exposing Pd to 2000 Torr for 20 min at 400 K, cooling to 80 K, and then pumping away the hydrogen gas. The sample prepared in this manner was directly inserted from the preparation chamber into the XPS instrument.<sup>36</sup> The XPS data should be much less sensitive to surface conditions than data produced using ultraviolet light [ultraviolet photoemission-spectroscopy (UPS)] because the mean free path for the excited electron is  $\sim 15$  Å

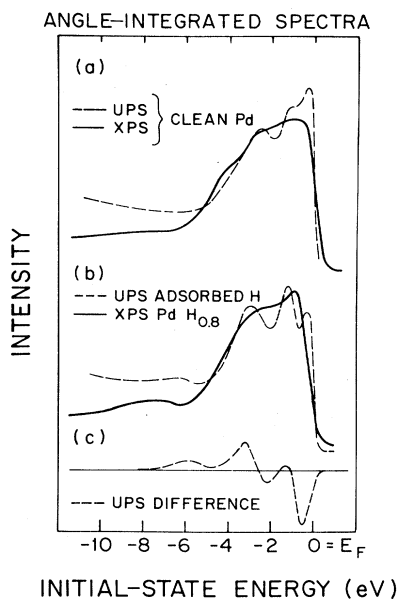


FIG. 11. Comparison of XPS spectra for Pd and PdH<sub>0.8</sub> (Ref. 36) with  $\vec{k}$ - and  $\hbar\omega$ -summed UPS spectra of Pd and Pd with adsorbed H.

at 1400-eV kinetic energy, while it may be as short as a few angstroms in the (50–100)-eV range.

The experimental data for PdH<sub>0.8</sub> when compared to clean Pd show the following changes induced by the hydrogen.<sup>36</sup>

(i) New states appear below the bottom of the clean Pd band. This weak feature is near  $-8$  eV in the curve shown in Fig. 11(b). The bottom of the Pd band is near  $-5$  eV as seen in Fig. 5.

(ii) The sharp edge near the Fermi energy in the PdH<sub>0.8</sub> spectrum has moved  $\sim 0.2$  eV away from the Fermi energy compared to the Pd spectrum.

(iii) The total width of the Pd band in PdH<sub>0.8</sub> is smaller than in Pd. Bennett and Fuggle<sup>36</sup> estimate a 10% band narrowing.

(iv) There is a small peak at  $\sim -1$  eV in the hydride spectrum which does not appear in the Pd spectrum.

Most of the observations described above are consistent with theoretical calculations of the electronic states of Pd and Pd hydride.<sup>37–41</sup> These calculations make the following predictions for Pd hydride.

(1) A new band is formed below the Pd bands as a result of the bonding of the H 1s electron with the Pd *d* electrons.<sup>41</sup> For the PdH<sub>0.8</sub> system, the calculation by Gelatt *et al.*<sup>39</sup> would predict a band approximately 3.5 eV wide with the bottom of the band at  $\sim -9$  eV.

(2) The *d* band of Pd is modified by the presence of the H and shifted down relative to the Fermi energy. The density of states at the Fermi energy in Pd hydride drops by a factor of 4 or 5 for large hydrogen concentrations.<sup>37,35</sup>

Bennett and Fuggle<sup>36</sup> explain the 0.2-eV shift in the leading edge of the PdH<sub>0.8</sub> valence-band spectrum as a consequence of the Pd *d* bands that are shifted down due to the presence of H [theoretical prediction (2)]. The approximately 3-eV-wide band near  $-8$  eV in curve *b* of Fig. 11 is the Pd-H split-off band predicted by theory. It is approximately in the correct energy position. The  $\sim 10\%$  narrowing of the Pd bands in PdH<sub>0.8</sub> is attributed to the  $\sim 3\%$  expansion of the Pd lattice and the new peak at  $-1$  eV in hydride spectrum is attributed to effects of spectrometer resolution.

The XPS data exhibited in Fig. 11 is at sufficiently high kinetic energy that it represents an integration over the SBZ. In contrast, our UPS data which we want to compare to the XPS data is angle resolved and taken in a low-photon energy range when small changes in  $\hbar\omega$  can produce large variations in relative intensities or peak positions. In an attempt to eliminate the  $\vec{k}$  and  $\hbar\omega$  dependence of spectra, a sum over collection angle and photon energy was performed. The two curves (dashed) shown in Fig. 11 are a result of summing the nine spectra shown in Figs. 2–4. The sum over three different values of *k* ( $\bar{\Gamma}, \bar{K}, \bar{M}$ ) should resemble an angle-integrated spectrum over the first SBZ and the sum over three photon energies should eliminate the effects of matrix-element variation in the amplitude of the individual peaks. These summed UPS spectra should be more sensitive to the surface than the XPS spectra.

Several qualitative features of the UPS spectra displayed in Fig. 11 are apparent. There is a H-induced band near  $-6$  eV in agreement with previously reported

angle-integrated spectra.<sup>16,17</sup> The Pd bandwidth seen in the UPS spectra is at least 0.5 eV narrower than the width observed in the XPS spectra. This is a consequence of the smaller density-of-states width for the surface of Pd compared to the bulk<sup>15</sup> (see Fig. 5). The high-surface density of states near the Fermi energy in clean Pd is removed and shifted to lower energy by the adsorption of H. This can more easily be seen in the difference curve plotted in C of Fig. 11. Finally, it should be noted that the split-off band for the bulk hydride is lower in energy than the equivalent surface band.

These qualitative observations can be made semiquantitatively by evaluating the first and second moments of the spectra. This requires that a background due to inelastically scattered electrons be subtracted from each spectrum. It is fairly obvious how to draw such a background curve through the data of Fig. 11, but there is no unique background curve. Our procedure was to use the same shaped curve for each set of data. Once the background had been subtracted, the first moment  $\bar{\epsilon}_0 = \sum \epsilon_i I_i / \sum I_i$  and the second moment  $\bar{\epsilon}_0^2 = \sum (\epsilon_i - \bar{\epsilon}_0)^2 I_i / \sum I_i$  were calculated. Table III lists the moments from the XPS and UPS data as well as the theoretical moments. The sum was only carried over the energy range of the Pd band, excluding the H split-off state. We are assuming that the XPS data samples reflect primarily the bulk while the UPS data reflect both the bulk and the surface. We stress again that the measured momenta are for the photoemitted electrons whose energy distribution has incorporated in it various matrix-element effects.

The first moment  $\bar{\epsilon}_0$  is a measure of the mean position of the occupied states and the second moment is a measure of the occupied density of states width. The shift in the occupied state center  $\bar{\epsilon}_0$  in going from Pd to Pd hydride is only  $\sim 0.1$  eV compared to  $\sim 0.25$  eV for the corresponding shift of the surface spectrum (see Table III). This small shift in the first moment of the Pd hydride band seems to contradict the obvious shift in the leading edge of the PdH<sub>0.8</sub> spectrum by 0.2 eV compared to the Pd spectrum. The explanation for this apparent discrepancy is the narrowing of the PdH<sub>0.8</sub> band compared to the bulk Pd band. The second moment  $\bar{\epsilon}_0^2$  in PdH<sub>0.8</sub> decreases by 18% compared to Pd. On the other hand, the adsorption of H onto the surface causes very little if any change in the surface Pd bandwidth ( $\sim 5\%$ ). There is a very marked

difference in the first and second moments of the XPS and UPS spectra for clean Pd. The first moment for the surface-sensitive UPS spectrum of Pd(111) is 18% smaller than the XPS spectrum [Fig. 11(a)], while the second moment is 24% smaller. Both of these observations are a result of the narrowing of the surface bands.

The theoretical numbers presented in Table III agree in the magnitude of the changes between bulk and surface or between a clean and a H-covered surface. For example, the theory predicts a 18% (22%) decrease in the first (second) moment for the surface of Pd compared to the bulk, in excellent agreement with the measured value of 18% (24%). The change in the surface bands, upon adsorption of H, shifts the first (second) moment by 26% (7%) compared to the experimental value of 13% (6%). The actual magnitude of the numbers is consistently too large by 5–13%. This undoubtedly is partially due to the fact that the photoelectron spectra does not sample the density of states that is calculated theoretically. The experimental curves probably weigh the *d* bands more heavily than the *s* bands.

The results of this section can be summarized.

- (1) An H-induced split-off state is present both for adsorbed H and Pd hydride. This state is lower in energy for the hydride than for the adsorbed H even though the adsorbed H is more tightly bound (Fig. 1).
- (2) The occupied Pd *d* density of states shifts away from the Fermi energy for both Pd hydride and adsorbed H. The shift in the first moment of the photoelectron spectrum is 4% for the bulk hydride and 13% for the adsorbed H.
- (3) The occupied Pd bandwidth decreases by 18% upon formation of PdH<sub>0.8</sub> while the surface Pd bandwidth for (1 $\times$ 1)H was almost the same as the clean-surface bandwidth.

### C. Room-temperature adsorption and conversion

The adsorption of H onto a Pd(111) crystal held at room temperature produces no observable change in the valence-band region of the photoemission spectra. Figure 12 shows a comparison of the effects on the clean spectra

TABLE III. First and second moments of spectra and density of states. (Energy sum only over Pd band.)

System	First moment (eV)	Second moment [(eV) <sup>2</sup> ]
XPS Spectra		
Pd	2.19	2.25
PdH <sub>0.8</sub>	2.27	1.84
UPS Spectra		
Pd(111)	1.79	1.7
(1 $\times$ 1)H on Pd(111)	2.03	1.6
Theory		
Bulk Pd	2.25	1.91
PdH	2.37	1.26
Pd surface	1.84	1.49
(1 $\times$ 1)H on Pd(111)	2.32	1.39

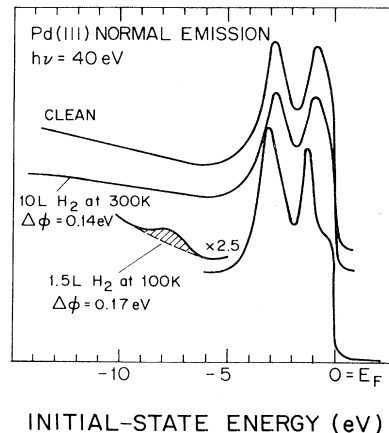


FIG. 12. Normal-emission photoemission spectra of clean and H-exposed surfaces at 100 and 300 K.

of a 1.5-L exposure at 100 K and a 10-L exposure at room temperature. The work-function changes are almost identical, and the work of Engel and Kuipers<sup>5</sup> indicates that the saturated H coverage at room temperature is approximately  $\frac{1}{2}$  of the saturated coverage at temperatures below 250 K. There is no split-off H state visible in the room-temperature spectrum, and more importantly, the surface state near the Fermi energy is not affected. Figure 10 showed that this surface state was sensitive to very small concentrations of H at a crystal temperature of 100 K, and the theoretical calculations indicate that the clean Pd surface state is destroyed for H adsorbed in any site.

This form of invisible H has "not been seen" on other transition-metal surfaces. Himpfel, Knapp, and Eastman<sup>42</sup> reported that H adsorbed onto Ni(111) at room temperature caused an enhancement in the intensity of the direct transition from the bulk *s* band. No split-off H bonding state was observed, even though these authors saw that H quenched a *s-p* surface state seen in normal emission. The explanation of this data was that a new type of chemisorption bond on a transition metal had been observed, where the bonding was predominantly with the free-electron-like *s* band. Low-temperature adsorption of H on Ni(111) produces a split-off state and destroys *d*-like surface states at the zone boundaries.<sup>10,43</sup> These *d*-like surface states are unaffected by adsorption of H at room temperature.

Smith<sup>44</sup> observed a reversible transition (with temperature) between an observable and invisible state of H on Nb. The temperature dependence of the intensity of the split-off H state was nearly linear going to zero around 700 K. Smith argued from the kinetics of the conversion process that it was not a bulk-surface exchange but instead a two-state chemisorption phenomenon with one state being invisible.<sup>44</sup> Recently, Greuter has shown that atomic hydrogen adsorbed onto Cu(111) also exhibits a split-off state which disappears irreversibly upon warming, before desorption occurs.<sup>45</sup>

In a preliminary report of this work as well as H adsorbed on Ni(111) and Pt(111), we had suggested that the invisible state was H in a subsurface site.<sup>10</sup> The primary argument supporting this model was the fact that subsurface H is not expected to affect localized *d*-like surface states of the clean surface,<sup>23,46</sup> but deeply penetrating *s-p*-like surface states can be quenched by this form of H.<sup>42,47</sup> Theoretical calculations for H and N bound under the first plane of Ti show that the localized *d* surface states are unperturbed.<sup>21,23,46</sup> The *s-p*-like surface states penetrate into the bulk so they are perturbed by subsurface impurities. This subsurface site is not physically unreasonable, since the energy difference between dissolved H and chemisorbed H has been attributed to the energy necessary to expand the metal lattice to accommodate the H,<sup>48</sup> i.e., approximately  $2.9 \text{ \AA}^3$  per H atom.<sup>1</sup> This energy is approximately 0.33 eV per H atom in Pd. If the surface plane is soft and it cost little energy to expand it, then the bonding energy of this site could be  $\sim 0.5 \text{ eV}$  (0.33 eV lower than the heat of solution). The major problem with this subsurface model is that there should be a H  $1s-M$  bonding level split off from the Pd band. The energy position of this level should be somewhere between the position seen for low temperature chemisorbed H and bulk hydrides. That means we should see this level in the energy

range of 7–9 eV depending upon its dispersion. The UPS data of Schlapbach and Burger for  $\text{PdH}_{0.6}$  show a weak feature at a binding energy of  $\sim +8 \text{ eV}$ .<sup>35</sup> The intensity of the hydride is approximately the same as seen in Fig. 10(b).

This invisible form of H is so common that it must be due to some general behavior of H on a variety of metal surfaces. It seems unsatisfactory to have a different explanation for each metal. For example, for Ni this phenomena could be attributed to H bonding into the *s* band as theory predicts,<sup>49</sup> but that surely would not explain Pd (Refs. 13 and 50) or Nb.<sup>44</sup> The data for Nb and Pd could, in principle, be explained as a surface-bulk exchange because H is soluble in the bulk, but this explanation would not work for Ni, Co, or Pt.

There are more experimental facts about this state or the conversion between the two states. First, the H in the room-temperature state is on or near the surface. The work-function change at saturation is 0.18 eV and the thermal-desorption spectra give a peak near 380 K. Figure 13 shows a wide energy scan of the same energy distribution shown in Fig. 12. The secondary electron-emission intensity and shape changes with the room-temperature adsorbed H, proving that the H is located within an electron mean free path of the surface, i.e.,  $< 10 \text{ \AA}$ . The second important observation concerns the conversion of the low-temperature phase. If the surface is heated,<sup>51</sup> after adsorption of H at 100 K there is no change until  $T \sim 250 \text{ K}$ , then the H split-off state starts to lose intensity. The split-off state is completely gone by 260–270 K and the clean-surface state is fully restored by 290 K. We have only done the detailed temperature study for high exposures ( $> 2 \text{ L}$ ) where the dispersion of the low-temperature state is fully developed. At this coverage our thermal-desorption spectra indicate that we have desorbed  $\sim \frac{1}{2}$  of the original layer by the time we reach 290 K. Low exposures of H at  $T = 100 \text{ K}$  also produce a split-off state and destroy the surface state (Fig. 10). Warming these low-coverage layers to room temperature converts all of the adsorbed H to the invisible state, without any desorption. This is an irreversible process, since cooling back to 100 K does not produce the initial spectrum.

Adsorption at low temperatures followed by warming to  $\sim 290 \text{ K}$  and subsequently cooling back down to 100 K does not restore the H-induced split-off state or destroy

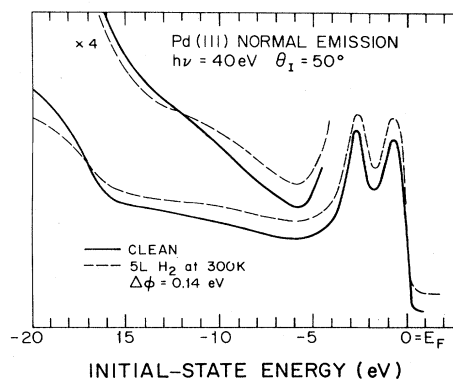


FIG. 13. Normal-emission photoemission spectra of clean and H-exposed Pd(111) surfaces at 300 K.

the surface states, independent of coverage. If a  $H(1 \times 1)$  low-temperature layer is warmed to 290 K, cooled back down, and reabsorbed, one obtains the identical photoemission and thermal-desorption spectra that the original low-temperature state exhibited. This means that either the ordered visible phase and the invisible phase coexist at 100 K, or that readsorption onto an invisible phase at 100 K converts it back to the visible ordered phase. Therefore we are left with two models: (1) a two-state chemisorption model, and (2) a density-dependent conversion. The saturation coverage at low temperature is different in the two models, i.e., one monolayer for the conversion model [model (2)] and approximately two monolayers for the two-state model [model (1)].<sup>52</sup> There are no absolute coverage measurements for H on Pd(111), but the same behavior is observed for H on Ni(111) (Ref. 10) and Narusawa<sup>27</sup> has measured the H coverage using a nuclear reaction. The saturation coverage is one monolayer within experimental error. Therefore the most reasonable explanation is that we are observing a density-dependent transition on Ni and Pd(111). This is consistent with the data of Engel and Kuipers<sup>5</sup> where they observed that the low coverage of H at 250 K was disordered, but as the coverage increased close to unity the layer ordered. One conspicuous problem with this model is the appearance of the split-off state in Fig. 11 at low coverages. The work-function change for the low-exposure curves of Fig. 10 indicated we had more H present than would be consistent with the intensity of the split-off state. We may not be in equilibrium, the phase diagram could be different at 100 K compared to 250 K, or the relationship between work-function change and coverage could be very nonlinear.

The previous paragraphs proposed a model for the observed changes in the photoelectron spectra with H coverage and substrate temperature. The nature of the low-temperature high-coverage state is well understood, but the microscopic details of the invisible state are still very uncertain. We know that the bond energy of the H to the Pd in this state must be slightly larger than the energy per H atom in the  $H(1 \times 1)$  structure, so there should be a split-off H state, and if the H is adsorbed, the Pd  $d$ -band surface states should be affected. How to reconcile these statements with the observed facts is the issue.

The density-dependent order-disorder conversion model predicts that the room-temperature phase in our experiment is disordered because the density is too low. If the H atoms in the disordered layer are moving rapidly or occupying a variety of sites, then the split-off state could have been smeared out over a 3- or 4-V range making it too weak to observe. This does not explain the observation that the  $d$  surface states are unaffected. Adsorption of molecules such as CO into disordered configurations on Pd(111) removes all of the surface states.

A subsurface H state which was disordered or moving rapidly, i.e., lattice gas, would explain all of the photoemission results, but it would be difficult to explain how the molecular-beam experiments could detect a disordered H layer under the surface.<sup>5</sup> Obviously, we need more experimental information: (1) Absolute coverage measurements as a function of crystal temperature and H-gas pressure; (2) structural information about the metal-metal interplanar spacing as a function of H coverage; (3) information about the phase diagram of H on these metals.<sup>53</sup>

#### IV. CONCLUSION

The nature of the H-Pd bonding for adsorption at low substrate temperatures has been described in detail using angle-resolved photoemission and theoretical calculations. The H forms an ordered  $(1 \times 1)$  structure as seen by the two-dimensional band dispersion (Fig. 5) with each H atom setting in a threefold site. The comparison of theory and experiment showed a high degree of sensitivity to the actual bonding coordination of the H, but less sensitivity to the H-Pd bond length. A good agreement was achieved for a bond length of 1.69 Å, which is the sum of covalent radii. The bonding is predominantly H  $1s$ -Pd  $4d$ , which produces a very localized surface bond. The bond is so localized that the theory showed no differences for the two types of threefold sites.

Adsorption of H at substrate temperatures above  $\sim 250$  K produced a form of H which is invisible in the direct photoemission spectra. This form of H, which is approximately  $\frac{1}{2}$  of the concentration achieved at 100 K, is located in the surface region, as witnessed by the changes in the work function and secondary electron emission, as well as in the thermal-desorption spectra. The conversion of the low-coverage, low-temperature visible adsorbed H to low-coverage room-temperature invisible H is irreversible.

Our proposed model for this system involves ordered adsorbed H at saturation coverage (the coverage is one monolayer) and subsurface H for the lower coverages ( $< \frac{1}{2}$ ). We believe that there is a reversible transition between these two phases at a coverage of  $\sim \frac{1}{2}$  of a monolayer.

#### ACKNOWLEDGMENTS

We would like to thank the staff of the Synchrotron Radiation Center of the University of Wisconsin for their support. This work was supported by the U.S. Office of Naval Research. The synchrotron beam line was funded and supported primarily by the National Science Foundation through the Materials Research Laboratories program at the University of Pennsylvania, under Grant No. DMR-79-23647.

\*Present address: Exxon Research and Engineering Company, P.O. Box 45, Linden, New Jersey 07036.

†Present address: Physics Department, University of California, Berkeley, California 94720.

<sup>1</sup>*Hydrogen in Metals I and II*, Vols. 28 and 29 of *Topics in Applied Physics*, edited by G. Alefeld and J. Volkl (Springer, New York, 1978).

<sup>2</sup>J. F. Lynch and T. B. Flanagan, *J. Phys. Chem.* **77**, 2628 (1977).

<sup>3</sup>See the references and arguments in the Introduction of Ref. 4.

<sup>4</sup>M. Kiskinou, G. Bliznakou, and L. Surnev, *Surf. Sci.* **94**, 169 (1980).

<sup>5</sup>T. Engel and H. Kuipers, *Surf. Sci.* **90**, 162 (1979).

<sup>6</sup>K. Christmann, G. Ertl, and O. Schober, *Surf. Sci.* **40**, 61

- (1973).
- <sup>7</sup>H. Conrad, G. Ertl, and E. E. Latta, *Surf. Sci.* **41**, 435 (1974).
- <sup>8</sup>R. J. Behm, K. Christmann, and G. Ertl, *Surf. Sci.* **92**, 320 (1980).
- <sup>9</sup>S. Andersson, *Solid State Commun.* **70**, 4168 (1979).
- <sup>10</sup>W. Eberhardt, F. Greuter, and E. W. Plummer, *Phys. Rev. Lett.* **46**, 1085 (1981).
- <sup>11</sup>The thermal-desorption spectra of H adsorbed on the (111) and (100) faces of Ni, Pd, and Pt at  $\sim 100$  K show, in general, a two-peak spectrum. Conrad (Ref. 12) has unpublished data for H on Pd(111) at low temperatures showing two peaks or a peak and a shoulder.
- <sup>12</sup>H. Conrad, Ph.D. thesis, University of Munich, 1975 (unpublished).
- <sup>13</sup>S. G. Louie, *Phys. Rev. Lett.* **42**, 476 (1979).
- <sup>14</sup>O. Blis and C. Calandra, *Surf. Sci.* **83**, 83 (1979).
- <sup>15</sup>S. G. Louie, *Phys. Rev. Lett.* **40**, 1525 (1978).
- <sup>16</sup>J. Demuth, *Surf. Sci.* **65**, 369 (1977).
- <sup>17</sup>H. Conrad, G. Ertl, J. Kuppers, and E. E. Latta, *Surf. Sci.* **58**, 578 (1976).
- <sup>18</sup>D. R. Lloyd, C. M. Quinn, and N. V. Richardson, *Surf. Sci.* **63**, 174 (1977).
- <sup>19</sup>Shang-Lin Weng and M. El-Batanouny, *Phys. Rev. Lett.* **44**, 612 (1980).
- <sup>20</sup>J. P. Muscat and D. M. Newns, *Surf. Sci.* **99**, 609 (1980).
- <sup>21</sup>P. J. Feibelman, D. R. Hamann, and F. J. Himpsel, *Phys. Rev. B* **22**, 1734 (1980).
- <sup>22</sup>D. E. Eastman, *Solid State Commun.* **10**, 933 (1972).
- <sup>23</sup>P. J. Feibelman, and D. R. Hamann, *Phys. Rev. B* **21**, 1385 (1980).
- <sup>24</sup>S. G. Louie, K.-M. Ho, and M. L. Cohen, *Phys. Rev. B* **19**, 1774 (1979).
- <sup>25</sup>M. Schluter, J. R. Chelikowsky, M. L. Cohen, and S. G. Louie, *Phys. Rev. B* **12**, 4200 (1975).
- <sup>26</sup>T. Narusawa, W. Gibson, and E. Tornqvist, *Phys. Rev. Lett.* **47**, 417 (1981).
- <sup>27</sup>T. Narusawa (private communication) saw no change in the angular profile along the channeling direction after H adsorption on Ni(111).
- <sup>28</sup>H adsorbed on Pt(111) at 185 K showed only a 1.3% outward expansion of the Pt(111) lattice; J. A. Davies, D. P. Jackson, P. R. Norton, D. E. Posner, and W. N. Unertl, *Solid State Commun.* **34**, 41 (1980).
- <sup>29</sup>See Ref. 10 for the comparison of W. Ho, J. DiNardo, and E. W. Plummer, *J. Vac. Sci. Technol.* **17**, 134 (1980) for Ni and A. M. Baro, H. Ibach, and H. D. Bruchmann, *Surf. Sci.* **88**, 384 (1979) for Pt.
- <sup>30</sup>M. A. Van Hove, G. Ertl, K. Christmann, R. J. Behm, and W. H. Weinberg, *Solid State Commun.* **28**, 373 (1978).
- <sup>31</sup>C. G. Olson, P. W. Lynch, and R. Rosei, *Phys. Rev. B* **22**, 593 (1980).
- <sup>32</sup>A 15% change in the H-Pd interplanar distance for site C results in a change of less than 0.1 eV in the position of the H 1s—Pd 4d bonding band.
- <sup>33</sup>See Ref. 37 for a review up to 1979 and Refs. 38—41 for more recent publications.
- <sup>34</sup>Much of the earlier work was not reproducible, see historical development in Refs. 37 and 36.
- <sup>35</sup>L. Schlapback and J. P. Burger, *J. Phys. (Paris) Lett.* **43**, L273 (1982).
- <sup>36</sup>P. A. Bennett and J. C. Fuggle, *Phys. Rev. B* **27**, 2145 (1983).
- <sup>37</sup>A. C. Switendick, *Z. Phys. Chem. Neue Folge* **117**, 89 (1979).
- <sup>38</sup>P. Jena, F. Y. Fradin, and D. E. Ellis, *Phys. Rev. B* **20**, 3543 (1979).
- <sup>39</sup>D. Gelatt, H. Ehrenreich, and J. Weiss, *Phys. Rev. B* **17**, 1940 (1978).
- <sup>40</sup>J. S. Faulkner, *Phys. Rev. B* **13**, 2391 (1976).
- <sup>41</sup>C. T. Chan and S. G. Louie, *Phys. Rev. B* **27**, 3325 (1983).
- <sup>42</sup>F. J. Himpsel, J. A. Knapp, and D. E. Eastman, *Phys. Rev. B* **19**, 2872 (1979).
- <sup>43</sup>F. Greuter and E. W. Plummer (unpublished).
- <sup>44</sup>R. J. Smith, *Phys. Rev. B* **21**, 3131 (1980); see also R. A. Johnson and G. J. Dienes, *ibid.* **21**, 3137 (1980).
- <sup>45</sup>F. Greuter and E. W. Plummer (unpublished).
- <sup>46</sup>P. J. Feibelman and F. J. Himpsel, *Phys. Rev. B* **21**, 1394 (1980).
- <sup>47</sup>F. Greuter has observed this invisible-type H on Co(0001) where an *s-p* surface state is affected by H adsorption, as it was on Ni(111) (Ref. 42).
- <sup>48</sup>M. A. Pick and D. O. Welch, *Bull. Am. Phys. Soc.* **336** (1981).
- <sup>49</sup>T. H. Upton and W. A. Goddard III, *Phys. Rev. Lett.* **42**, 472 (1979).
- <sup>50</sup>R. P. Messmer, D. R. Salahub, K. H. Johnson, and C. Y. Yang, [*Chem. Phys. Lett.* **51**, 84 (1977)] have calculated the bonding of H to four-atom tetrahedral and six-atom octahedral Ni, Pd, and Pt clusters showing that the *d* bonding to the H is much more important in Pd and Pt than Ni.
- <sup>51</sup>We raised the temperature to some value *T* for 10 sec than cooled it down and recorded the spectrum.
- <sup>52</sup>Our thermal desorption as well as the molecular scattering data of Engel and Kuipers (Ref. 5) indicated that  $\sim \frac{1}{2}$  of the saturated low-coverage layer is desorbed by heating to  $\sim 300$  K. We assume that the H(1 $\times$ 1) state we see is one monolayer.
- <sup>53</sup>B. J. Behm, K. Christmann, and G. Ertl have produced a partial phase diagram for H on Pd(100), *Surf. Sci.* **92**, 320 (1980).